Comparative Characteristics of Membrane-Active Single-Chained Ether Phospholipids: PAF and Lyso-PAF in Langmuir Monolayers

ARTICLE *in* THE JOURNAL OF PHYSICAL CHEMISTRY B · MARCH 2012

Impact Factor: 3.3 · DOI: 10.1021/jp2121092 · Source: PubMed

4 AUTHORS, INCLUDING:

Michał Flasiński
Jagiellonian University
36 PUBLICATIONS **181** CITATIONS
SEE PROFILE

Paweł Wydro
Jagiellonian University
53 PUBLICATIONS **624** CITATIONS
SEE PROFILE

Patrycja Dynarowicz-Latka
Jagiellonian University
177 PUBLICATIONS **1,951** CITATIONS
SEE PROFILE

THE JOURNAL OF PHYSICAL CHEMISTRY B

Article

pubs.acs.org/JPCB

Comparative Characteristics of Membrane-Active Single-Chained Ether Phospholipids: PAF and Lyso-PAF in Langmuir Monolayers

Michał Flasiński,* Marcin Broniatowski, Paweł Wydro, and Patrycja Dynarowicz-Łątka

Faculty of Chemistry, Jagiellonian University, Ingardena 3, 30-060 Kraków, Poland

ABSTRACT: 1-*O*-Octadecyl-2-acetyl-*sn*-glycero-3-phosphocholine (PAF) and its deacetylated precursor (lyso-PAF) are membrane-active single-chained ether phospholipids, which play an important signaling role in different physiological processes. There is strong evidence that one of the possible mechanisms of PAF and lyso-PAF activity is connected with their direct influence on biomembranes. Although both lipids have very similar structure, their biological activity is very different and in some cases even antagonistic. Unfortunately, there is a lack of the studies correlating these observations with the molecular structure of both compounds. Therefore, we decided to apply model systems and advanced physicochemical methods to explore this subject and look for the reasons of the observed discrepancies. As a model system, we prepared Langmuir monolayers of PAF and lyso-PAF at the air/water interface. The physicochemical characteristic of the model membranes under different experimental conditions was performed with the application of the Langmuir monolayer technique, Brewster angle microscopy, and the methods based on synchrotron radiation scattering (XR and GIXD). Both compounds form stable Langmuir monolayers, in which the lipid molecules are strongly immersed into the water subphase. The monolayers have expanded character, meaning that the hydrophobic tails are considerably tilted and disordered. Similarly to biochemical studies, also in our model systems, profound differences in the properties of PAF and lyso-PAF were observed. Contrary to PAF, the lyso-PAF molecules express the propensity to form organized, periodical structures in the model membranes. It is manifested in the phase transition observed in the course of the lyso-PAF π–A isotherm which was correlated with the diffraction signal registered with the application of the GIXD method. The formation of 2D domains of hexagonal ordering of the film forming molecules was observed only for the lyso precursor. The observed differences between PAF and lyso-PAF were explained taking into consideration the chemical activity of the free hydroxyl group present in the headgroup of the latter molecule. The formation of hydrogen bonds between the lyso-PAF molecules as well as the stronger hydration of its hydrophilic fragment can be the key factor differentiating the activity of PAF and lyso-PAF in the investigated systems as well as in the native biomembranes.

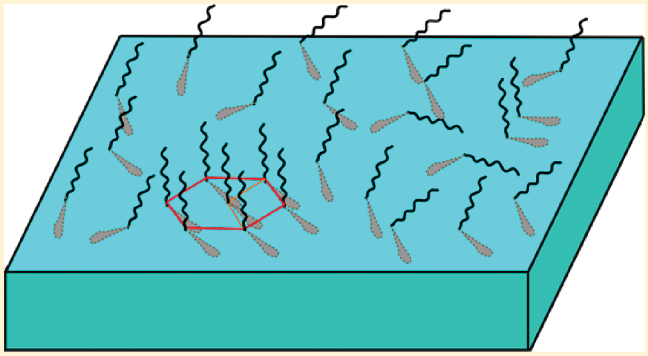

INTRODUCTION

For many years, phosphoglycerides together with sphingolipids and sterols were known to be elementary building blocks of biological membranes. Nowadays, it is evident that this class of substances apart from its structural significance perform also important signaling and regulatory functions.[1,2] Among phospholipids, a special place belongs to the group of ether phosphoglycerides in which the glycerol backbone is substituted by only one (in lyso-phospholipids) or two hydrocarbon chains via an ether linkage.[3] Interesting representatives of single-chained ether phospholipids are platelet activating factor (PAF) and its deacetylated precursor lyso-PAF. Naturally occurring PAF is an ether analogue of phosphatidylcholine, possessing a single, predominantly C_{16} or C_{18} hydrocarbon chain connected by an ether linkage at the glycerol C1 carbon, while the substituent at the C2 carbon is an acetate unit.[4] Historically, platelet aggregation caused by this ether lipid was the first phenomenon described in the literature, proving its biological activity.[5] However, it was later identified to also be a mediator of inflammation in addition to its involvement in the mechanism of the immune response.[6] PAF is not stored in cells, but it is synthesized, in response to various stimulations, by platelets, leukocytes, endothelial cells, and mast cells.[4,7−9]

Its inactive precursor is 1-*O*-alkyl-2-acyl-glycerophosphocholine, which under the influence of phospholipase A2 is hydrolyzed to a fatty acid (usually arachidonic) and lyso-PAF. Lyso-PAF is then acetylated by a specific acetyltransferase into active PAF (Scheme 1).[10,11]

PAF is connected with many important inflammatory processes like, for example, edema formation,[12] endotoxic shock,[13] hyperpermeability in microvessels,[8,14] and angiogenesis.[15] Interestingly, the proangiogenic and proinflammatory activity caused by PAF is identified as a factor which can induce tumor tissue growth and proliferation.[15−19] It is worth mentioning that PAF is also implicated in pulmonary diseases (e.g., asthma) and atherosclerosis.[11,20−23] Moreover, PAF is involved in

Received: December 15, 2011
Revised: February 7, 2012
Published: February 8, 2012

   dx.doi.org/10.1021/jp2121092 | *J. Phys. Chem. B* 2012, 116, 3155−3163

Scheme 1. Pathway of PAF Synthesis

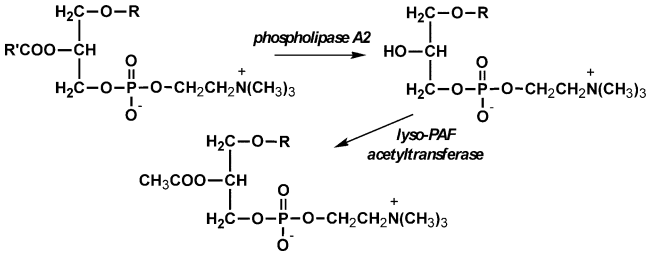

vascular barrier regulation; that is, it can accumulate in endothelium and subendothelial structures which lead to the morphological and biochemical changes of endothelial cells.[8,24]

Although both PAF and lyso-PAF have very similar chemical structures, their physicochemical properties, biological function, and consequently mode of action are markedly different. There is strong evidence that PAF is biologically more potent than its lyso-precursor. Bussolino and co-workers investigated the influence of lyso-PAF and PAF on the endothelium cell shape induced by both single-chained phospholipids.[6] It turned out that lyso-PAF in the concentration about 10^4 times greater than the minimal active concentration of PAF was completely ineffective. Moreover, another study suggests that, in contrast to PAF, lyso-PAF has no influence on the cytosolic free calcium concentration.[25]

Moreover, in the literature, there are also examples of studies demonstrating that PAF and its lyso-precursor reveal effects comparable in strength but opposing in character. Namely, Welch demonstrates an antagonistic effect of the discussed phospholipids in the activation of neutrophils and platelets which is connected with NADPH oxidase promotion by PAF and inhibition by lyso-PAF.[26] It should be stressed that the aforementioned differences in the properties, function, and activity of both ether phospholipids are very important; nonetheless, there is an evident gap in the literature concerning this issue. Namely, still relatively little is known about the correlation between the well documented physiological activities of these ether lipids and their physicochemical properties at the molecular level. Unfortunately, scientific data in this case is rather fragmentary and inconsistent; therefore, to shed light onto this problem, we planned to carry out systematic studies in this field.

In our experiments, we apply the Langmuir monolayer technique which serves as an excellent model environment to study the properties of insoluble surfactants, in particular phospholipids.[27−29] The application of this method complemented with modern physicochemical techniques enables us to perform detailed analysis regarding the behavior of the investigated lipids at the air/water interface. The undertaken experiments are focused on seeking the relationship between the physicochemical properties of both ether lipids and their different bioactivities.

The strong argument supporting the studies in a membrane mimicking environment is the fact that, although a broad range of PAF bioactivity is mediated by the highly specific G protein-coupled receptor (PAF-R) localized in a cellular membrane, some important effects exerted by PAF occur by a receptor independent mechanism.[30] A good example here is the pro-apoptotic activity of PAF described in several articles;[31,32] nonetheless, the exact mechanism of this effect still remains unclear.[33] It is noteworthy that PAF and lyso-PAF can be easily incorporated into lipid membranes and, in consequence, alter their properties.[9,34] Mrówczyńska et al. investigated the influence of C_{16}PAF on human red blood cell membranes, and the results of these studies reveal that PAF can be easily accumulated into outer membrane leaflet, leading to the distinct erythrocyte shape alterations.[35] Similar results were also acquired by Chen an co-workers, leading to the conclusion that PAF can be accumulated in the membrane of unstimulated neutrophils.[9]

The aforementioned studies expose the receptor-independent mechanism of PAF action and also indicate that cellular membranes are the primary target for bioactive compounds, such as ether phospholipids. This mechanism was proved on the example of another structurally similar, but in contrast to PAF and lyso-PAF, synthetic single-chained ether phospholipid, edelfosine, which is known to exert anticancer activity.[36−38]

Herein, we focus special attention on the physicochemical properties of C_{18}PAF and C_{18}lyso-PAF in monomolecular layers at the air/water interface, since, to the best of our knowledge, this has not been investigated so far in contrast to double-chained membrane phospholipids, which have been intensively investigated in 2D systems.

In our research, we applied the classical Langmuir monolayer technique complemented with modern physicochemical methods to characterize the behavior of C_{18}PAF and C_{18}lyso-PAF at the air/water interface. Basic information was acquired directly from the course of surface pressure (π) vs mean molecular area (A) isotherms as well as from stability experiments (both in static and dynamic approach). Moreover, to have insight into the organization of these single-chained lipid molecules in monolayers, we applied the synchrotron X-ray reflectivity technique (XR). This method provides information regarding electron density distribution in the direction perpendicular to the water surface, which enables the determination of monolayer thickness as well as interfacial roughness. Conclusions regarding monolayer structure and in-plane ordering were also drawn from the results obtained with the application of the grazing incidence X-ray diffraction technique (GIXD). Additionally, in our investigations, Brewster angle microscopy (BAM) was applied for direct visualization of the investigated film structures.

The results presented in this paper provide new information regarding film-forming properties of two single-chained ether phospholipids, PAF and lyso-PAF, underlining especially subtle differences between those lipids.

EXPERIMENTAL SECTION

Materials. The investigated single-chained phospholipids, namely, C_{18}PAF (1-*O*-octadecyl-2-acetyl-*sn*-glycero-3-phosphocholine) and C_{18}lyso-PAF (1-*O*-octadecyl-*sn*-glycero-3-phosphocholine), of the highest purity available in stock (99%) were purchased from Bachem AG Switzerland and used without further purification. A spreading solution of the lipids of a concentration close to 0.2 mg/mL was prepared in a chloroform/methanol 9/1 (v/v) mixture. Chloroform of spectroscopic purity (99.9% stabilized by ethanol) as well as methanol (99%) were provided by Sigma-Aldrich. In all experiments on the Langmuir trough, ultrapure water of resistivity $\geq$18.2 MΩ·cm^{-1} from Milli-Q was applied as a subphase.

Methods. *Langmuir Experiments.* In routine experiments, $\pi-A$ isotherms and stability measurements were recorded with the NIMA (Coventry, U.K.) Langmuir trough of a total area of 300 cm^2 equipped in a single movable barrier placed on an antivibration table. The surface pressure was

dx.doi.org/10.1021/jp2121092 | J. Phys. Chem. B 2012, 116, 3155−3163

measured with an accuracy of 0.1 mN/m using a Wilhelmy balance equipped with a surface pressure sensor made of filter paper (ashless Whatman). The required amounts of lipid solutions were spread on a pure water surface with a Hamilton microsyringe precise to 2 μL. In each experiment, the monolayer was left to equilibrate for at least 5 min before the monolayer compression was initiated with the barrier speed of 20 cm^2/min (~12 Å^2/molecule·min). The circulating water system was used to control the subphase temperature.

BAM Visualization. The investigated monolayers were visualized with an ultraBAM apparatus (Accurion GmbH, Göttingen, Germany). The light source was a 50 mW laser emitting p-polarized light of a 658 nm wavelength direct to the air/water interface at the Brewster angle (53.2°). The lateral resolution of the BAM image was 2 μm. The microscope was installed over a KSV (Helsinki, Finland) double barriers Langmuir trough, model 2000 of total area 700 cm^2. The temperature of the subphase (20 °C) was regulated thermostatically to within 0.1 °C. The surface pressure was monitored during the experiment with the Wilhelmy plate made of filter paper (ashless Whatman). In all experiments, at least 5 min were allowed for the spreading solvent to evaporate after which the symmetrical compression was initialized with the barrier speed of 20 cm^2/min.

X-ray Reflectivity Measurements. Synchrotron X-ray reflectivity (XR) measurements for the investigated single-chained phospholipids were performed with the liquid surface diffractometer at the BW1 beamline in HASYLAB, DESY synchrotron center (Hamburg, Germany). The incidence X-ray wavelength of λ =1.303 Å was obtained by the reflection from a beryllium (200) monochromator crystal. In the Langmuir monolayer experiment, a single barrier trough of total area 600 cm^2 (R&K, Potsdam, Germany) placed in a gastight container mounted on the goniometer of the diffractometer was used. The surface pressure measurements were carried out with the Wilhelmy balance equipped with a filter paper stripe as a surface pressure sensor. The constant temperature during measurements (20 °C) was controlled thermostatically by the circulating bath system.

In each experiment after spreading the lipid solution on the water surface, the container cover was sealed and the canister was flushed with helium in order to reduce the oxygen level. The purpose of this procedure is to minimize the beam damage during reflectivity scans and reduce the scattering background. After at least 40 min, the monolayer was compressed to the target surface pressure (30 or 35 mN/m), which was held constant during the entire experiment.

Both the construction of the BW1 beamline and the detailed theoretical background of the X-ray reflectivity technique were described in an exhaustive manner in several previous articles;[39−43] thus, we focus here only on the principal information.

According to the definition, reflectivity R is described as the intensity ratio of X-rays specularly scattered from an interface relative to the incident beam intensity. Reflectivity is measured as a function of momentum transfer vector Q_z in accordance with the equation

$$Q_z = |k_{out} - k_{in}| = \frac{4\pi}{\lambda}\sin(\alpha)$$

where λ is the wavelength of incident X-ray beam and $\alpha = \alpha_i = \alpha_f$ is the angle equal to the both incident (α_i) and reflected (α_f) angles. The experimental $R(Q_z)$ curve can be measured by a NaI scintillation detector moving on the α_f arc.[39]

From the measurements of specular reflectivity, the detail information concerning the laterally averaged electron density distribution (ρ) along the direction perpendicular to the monolayer plane can be obtained. It is performed by modeling the deviation of measured X-ray reflectivity from the Fresnel law for the ideally sharp interfaces.[42] In analysis of our results, we applied the electron density model based on the construction of a stack of homogeneous slabs ("boxes") with an assumption that each box possesses constant electron density and thickness.[39] The boundaries between adjacent slabs were smeared out with a Gaussian function of standard deviation σ to account for the roughness of interfaces caused by the thermally excited microscopic capillary waves and atomic interface roughness. Simulation of the reflectivity profile was carried out using the Parratt32 software application by the Hahn-Meitner Institute, Berlin. This package is based on Parratt's recursive algorithm for stratified media using independent layers.[44] For our purpose, we decided to apply the model with two independent boxes as an optimal assumption of the single-chained phospholipid's monolayer. The first box contains the hydrophobic part of the molecule, that is, the acyl chain, whereas the second one includes the polar headgroup and adjacent water molecules. In the routine procedure, the parameters fitted were slab thicknesses, electron densities, as well as the interfacial roughness. The results of the best fitting models with the lowest χ^2 values were taken for the discussion in the next section.

Grazing Incidence X-ray Diffraction (GIXD). GIXD experiments were performed using the same apparatus, as described above in the case of the XR method. The comprehensive theoretical description of the GIXD technique as well as the procedure of data processing were described in detail both in our previous papers[45−48] and in several other articles.[39,41,42,49] GIXD measurements provide high resolution information about the lateral organization of a monolayer on the Å scale. The quantitative information can be obtained only if there is a periodical ordering of surfactant molecules in a monolayer. If this requirement is fulfilled, the incidence X-ray radiation is scattered and therefore its intensity can be measured by a position sensitive detector (PSD). Afterward, the intensity is represented as a function of horizontal scattering vector (q_{xy}) and the scattering vector component along the vertical z coordinate (q_z) resulting in detection of Bragg peak(s) and Bragg rod(s), respectively. On the other hand, lack of the signal in the GIXD experiment is also valuable information, since it indicates that film-forming molecules are poorly organized in the monolayer plane and do not form a two-dimensional ordered phase.

RESULTS AND DISCUSSION

Figure 1 presents π−A isotherms registered for Langmuir monolayers of the investigated single-chained phospholipids together with the compression modulus dependency, defined as $C_s^{-1} = -A(d\pi/dA)$ versus π.[50] As far as the PAF isotherm is concerned, the surface pressure starts to rise at a molecular area of ca. 150 Å^2/molecule and collapses at ~40 mN/m, which corresponds to the mean molecular area of 45 Å^2/molecule (see Table 1).

The course of the π−A isotherm reveals that the monolayer is in a liquid expanded (LE) state, which can be quantitatively confirmed by the calculated C_s^{-1} values.[50] It should be also pointed out that both the course of the curves and the values of

dx.doi.org/10.1021/jp2121092 | J. Phys. Chem. B 2012, 116, 3155−3163

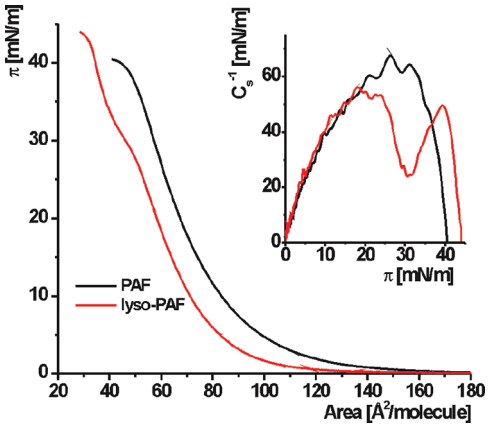

Figure 1. π–A isotherms of the investigated lipid films: PAF and lyso-PAF at 20 °C. The inset shows C_s^{-1}–π curves calculated from the corresponding compression isotherms.

Table 1. Parameters Characterizing the π–A Isotherms and C_s^{-1}–π Curves at 20 °C

	max C_s^{-1} (mN/m)	A_0 (Å²/molec)	A_{lim} (Å²/molec)	π_{coll} (mN/m)	A_{col} (Å²/molec)	ESP (mN/m)
PAF	68	150	87	40	45	33.5
lyso-PAF	57	124	80	44	31	32.5

molecular area parameters, such as A_0 and A_{lim}, are typical for surfactants bearing a bulky hydrophilic group and a tail with small cross-sectional area. Such surfactants form highly compressible monolayers in which molecules are tilted from the surface normal;[51] therefore, the hydrophobic interactions among them are weaker than in the case of perpendicularly oriented molecules which tend to pack closely in condensed domains. The π–A isotherm of lyso-PAF is significantly shifted toward lower mean molecular areas, and this is the first striking difference observed by us, as far as Langmuir monolayers of PAF and lyso-PAF are compared. As both compounds have the same hydrophobic chain, the differences must originate from the structure of the headgroup. Lyso-PAF possesses a free hydroxyl group at the glycerol C2 atom, whereas in PAF this group is acetylated. The acetylation can increase the bulkiness of the headgroup, resulting in the appearance of an additional conformational energy barrier as well as a slight decrease in its hydrophilicity. However, this group is small and it can be supposed that the formation of hydrogen bonds by the free −OH groups of two adjacent head-groups as well as between this group and the water molecules of the subphase is quite important here. Formation of additional hydrogen bonds between the hydroxyl group of lyso-PAF and water molecules can be a factor differentiating this compound from PAF. To verify our hypotheses and to have a broader view of this problem, the influence of subphase temperature on the course of π–A isotherms was investigated.

Figure 2 illustrates the influence of subphase temperature on the investigated monolayers' properties.

It is evident that both lipids demonstrate considerably different behavior in their monolayers when the temperature of the aqueous subphase is changed. In the case of PAF, three different values of temperatures were examined, namely, 10, 20, and 35 °C. One can find that this parameter slightly affects the course of the isotherm, as it was shown in Figure 2a. The

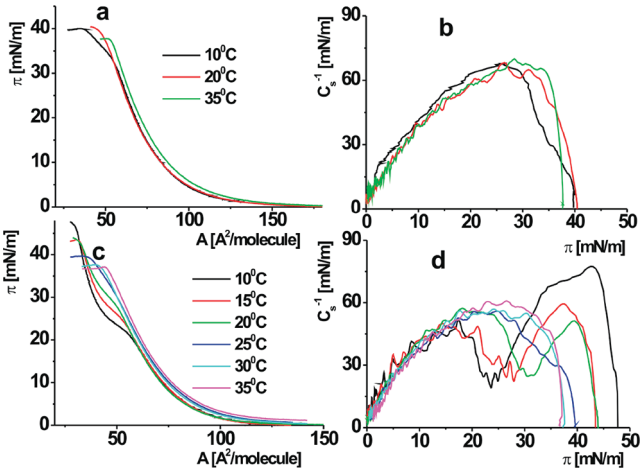

Figure 2. The π–A isotherms registered for PAF (a) and lyso-PAF (c) monolayers compressed on the water subphase at different temperatures. Graphs b and d present the compression modulus vs surface pressure (π) dependencies calculated from the π–A isotherms of PAF and lyso-PAF monolayers, respectively.

differences can be found only in the highest values of surface pressures, while the course of the π–A isotherms and therefore the calculated values of compression modulus are very similar. The situation is completely different as far as the lyso-PAF monolayer is concerned (see Figure 2c). The course of lyso-PAF isotherm measured at 10 °C proves that there is a distinct phase transition beginning at ca. 20 mN/m. With the increase of temperature, the plateau region of the isotherm shifts to higher surface pressure values; at 20 °C it can be described rather as a kink than a plateau, while at 25 °C it completely disappears. It is difficult to propose the mechanism of this transition only on the basis of the π–A isotherm course, but we will come back to this phenomenon in the discussion of the GIXD data. It should be emphasized here that the presence of the phase transition at lower temperatures is another characteristic in which the monolayers of PAF and lyso-PAF differ considerably.

Additional information can be extracted from the analysis of BAM images registered for monolayers of PAF and lyso-PAF (Figure 3). It can be seen that, at the surface pressure π = 0 mN/m, the 2D foam-like structures appear in images registered for both lipids. Such structures are characteristic for the coexistence of gas and liquid expanded state.[52,53] After compression was initialized, both films become homogeneous. Moreover, in the case of lyso-PAF, no signs of phase transition could be observed. Small, scattered bright spots appear at the surface only after the surface pressure reaches a value of ca. 36 mN/m and are visible in the images until the end of the compression. The existence of such bright structures is often related to the formation of a 3D phase on the surface, and it may reflect the monolayer's collapse.[53,54] To obtain additional information concerning the behavior of lipid molecules in surface films, the relaxation experiments were performed (Figure 4).

The stability tests were carried out in two different modes. Namely, in the first, so-called static stability experiment, the monolayer was compressed to the desired surface pressure (30 mN/m for a monolayer of PAF as well as 20 and 35 mN/m for lyso-PAF) and then the further compression was stopped. After that, at the constant molecular area, the surface pressure decay was monitored as a function of time. It can be seen that both monolayers compressed to a surface pressure of 20 and

dx.doi.org/10.1021/jp2121092 | J. Phys. Chem. B 2012, 116, 3155–3163

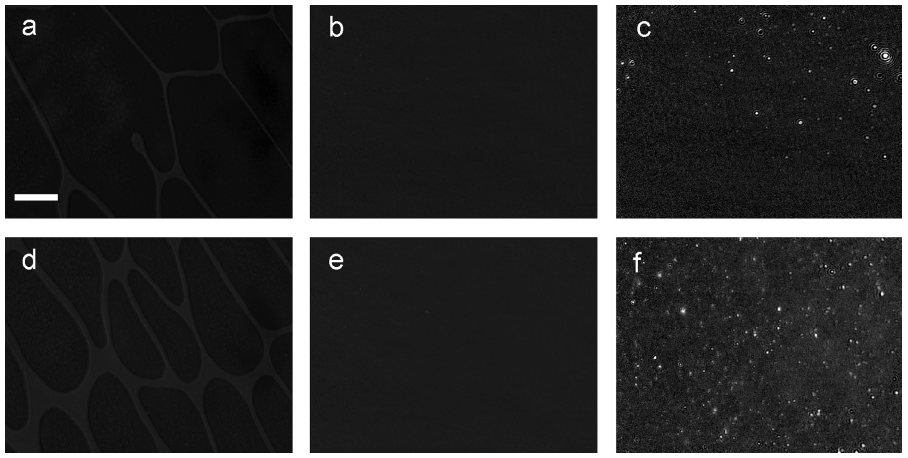

Figure 3. BAM images registered for the investigated monolayers of PAF (a–c) and lyso-PAF (d–f) at different stages of the compression at 20 °C: (a, d) π = 0 mN/m; (b, e) π = 25 mN/m; (c, f) π = 36 mN/m. The white bar indicates 100 μm.

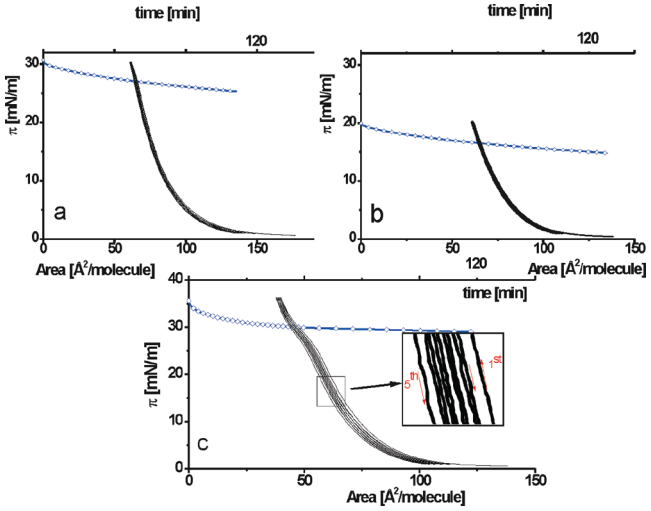

Figure 4. Static and dynamic stabilities of the investigated monolayers of PAF compressed to the surface pressure of 30 mN/m (a) and lyso-PAF: 20 mN/m (b) and 35 mN/m (c). The experiments were performed at 20 °C.

30 mN/m, respectively, have comparable stability; that is, the surface pressure decreases after ca. 90 min of about 15% of the initial values. High stabilities of the investigated monolayers were also confirmed in dynamic stability experiments in which five compression/expansion cycles were performed. It can be seen that the curves registered for the monolayer of PAF during compression and expansion cycles have very similar course. It means that the lipid molecules in monolayers compressed to such surface pressures neither desorb from the surface film nor form a 3D phase. This situation is typical for the surfactants forming expanded, highly compressible Langmuir monolayers in which well organized condensed domains do not form.[55] Comparable results were obtained also for the monolayer of lyso-PAF compressed to the surface pressure of 20 mN/m (Figure 4b). On the other hand, in the case of the experiment performed on the lyso-PAF monolayer above the phase transition region (π = 35 mN/m), it can be seen that the recorded narrow hysteresis loops are shifted slightly toward smaller molecular area in the subsequent cycles. This result indicates that the monolayer at this stage of compression reveals lower stability. The decrease of the film stability can be caused by the formation of multilayer domains. It can be promoted by the presence of the free hydroxyl group in the lyso-PAF molecule. The postulated hydrogen bond formation increases the intermolecular interaction, facilitating the 3D crystallization in the Langmuir monolayer.

An additional parameter which is often estimated in the discussion of Langmuir monolayer stability is equilibrium spreading pressure (ESP). ESP is the value of a surface pressure at which, under given thermodynamic conditions, two-dimensional monomolecular film is in equilibrium with the 3D bulk phase.[56] The values of ESP obtained in our experiments are very close to each other, i.e., 33.5 and 32.5 mN/m for PAF and lyso-PAF, respectively. As the collapse of monolayers of both investigated compounds is observed at higher surface pressures (ca. 40 mN/m), the monolayers can be treated as metastable in the surface pressure range between ESP and collapse pressure, which is a satisfactory explanation of the appearance of bright spots in BAM images observed also below the collapse pressure. The surface pressure value of ca. 30 mN/m is often acquired as corresponding to the conditions present in typical biomembranes. Monolayers of PAF and lyso-PAF are considerably stable also at this pressure value, which is a good prognostic for future investigation of these active ether lipids in model phospholipid membranes as well as beneficial for all experiments in which lipid layers are transferred on solid substrates.

The above-mentioned experiments can be considered as a general characterization of the investigated monolayers. They give important information about the biologically active ether lipids in the model systems; however, they do not provide facts regarding the orientation of the film-forming molecules in the angstrom scale. To gain such information, we applied synchrotron radiation and used the methods accessible on a liquid phase diffractometer, i.e., XR and GIXD.

X-ray reflectivity measurements were performed for Langmuir monolayers compressed to the surface pressure of 30 mN/m. Good stabilities of both films proved in the relaxation tests were a good prognostic for the high quality scans in these experiments. Additionally, in the case of lyso-PAF, reflectivity measurements were also performed for the monolayer compressed to the surface pressure of 35 mN/m on aqueous subphase cooled to 10 °C to get insight into the origin of the phase transition observed under such experimental conditions.

dx.doi.org/10.1021/jp2121092 | J. Phys. Chem. B 2012, 116, 3155–3163

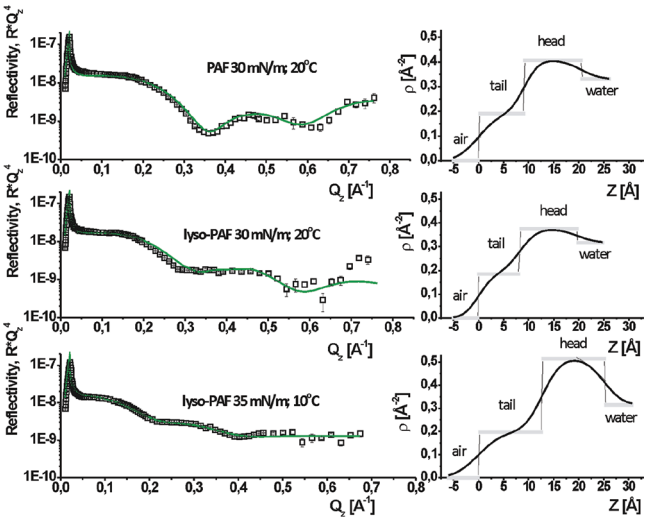

Figure 5. Normalized X-ray reflectivity curves for PAF and lyso-PAF monolayers and corresponding electron density (ρ) profiles calculated from the best fitting models. The reflectivity curves were multiplied by Q_z^4 in order to emphasize the differences.

The reflectivity curves for both single-chained phospholipids are presented in Figure 5. The graph contains experimental points together with the error bars as well as continuous curves obtained from the fitting procedure. Comparing these results, one can find that the reflectivity curves differ in the region of Q_z between ca. 0.25 and 0.60 Å^{-1}, which is caused by the differences in molecular orientation of these lipids at the air/water interface. In order to attain important parameters concerning the behavior of PAF and lyso-PAF in Langmuir monolayers, the reflectivity data were modeled using the Parratt algorithm. The best results (the lowest value of χ^2) were obtained for the two-slab model in which the first box refers to the region of the hydrophobic tail (lower value of electron density), whereas the second contains the polar headgroup with hydrating water molecules (higher ρ values). Such a division of phospholipid molecules into two boxes was successfully applied in our previous studies[46,47] as well as also frequently applied by the other authors.[49,57−59] The parameters derived from such a model were listed in Table 2.

Let us first discuss the values of calculated slab thicknesses. As it can be observed, the length of box 1 is 8.33 and 9.79 Å for a monolayer of PAF and lyso-PAF compressed on the water subphase of 20 °C, respectively. Although these values are different, the calculated numbers of electrons in both boxes are similar, i.e., 77 vs 84. It means that, in box 1, 10 carbon atoms are present (10 C), namely, 9 CH_2 groups and 1 terminal CH_3 group. Assuming that the length of hydrocarbon chain in its all-trans conformation can be calculated from the following equation: $L = (n + 9/8)\cdot 1.265$ Å, where n is the number of methylene groups and 9/8 is a correction for terminal CH_3,[60] the tail in these cases is significantly tilted from the axis perpendicular to the air/water interface. Taking into account the parameters obtained from reflectivity data, we are able to illustrate schematically the organization of both lipid molecules at the air/water interface (Figure 6).

As can be noticed, both lipid molecules are strongly immersed into the water subphase, namely, the eight-atom fragment of the hydrocarbon chain is penetrated by the water molecules and therefore it was located in the second box containing the hydrophilic part. For that reason, the head regions in both cases have high electron densities. Moreover, the number of electrons exceeds by about 58 and 42 the number of electrons calculated from the chemical formulas of PAF and lyso-PAF, respectively, which indicates that on average ∼6 and ∼4 water molecules are present in the second slab. This is not surprising, since the bent headgroup can easily accommodate small water molecules inside its spacious box. For comparison, based on neutron reflectivity measurements, it was found that the DPPC molecule in its head region holds on average four water molecules at a surface pressure of 35 mN/m.[61] The pictures in Figure 6 can suggest the presence of a more numerous representation of water molecules; however, when the real volumes (van der Waals spheres) of the atoms are considered, it becomes evident that the estimations made by the application of the Parratt algorithm are reasonable. It is not depicted in the picture, but it should be taken into consideration that the part of the hydrophobic chain having contact with water molecules is much more prone to *gauche* defects than the moiety present in the first slab.

The results described herein also indicate that, in the case of single-chained ether lipids, the orientation of molecules in the monolayer is slightly different as compared with the results obtained for structurally very similar lyso-PC,[47] in which the hydrocarbon chain is attached to the glycerol backbone by an ester bond. This structural discrepancy affects the electron density distribution in the boxes; namely, in the mentioned example, only the 6-atom fragment is immersed in the aqueous subphase.

Additionally, reflectivity measurements were carried out for the monolayer of lyso-PAF compressed to 35 mN/m on a water subphase at 10 °C (Figure 5).

It is evident that in this case the calculated thickness of box 1 is bigger than that for the same monolayer investigated at the lower surface pressure as well as at higher subphase temperature. At the same time, the electron density values in both cases differ only by ca. 0.01 Å^{-1}, which means that box 1 accommodates a hydrocarbon chain of 11 carbon atoms. Therefore, the difference is only in one methylene group.

It is also worth mentioning that, as far as the electron density in the second box is concerned, it turned out that at lower temperature the head region (box 2) accommodates on average

Table 2. Parameters Obtained from the Fitting of X-ray Reflectivity Curves[a]

	tail (box 1)					head (box 2)				
				number of electrons					number of electrons	
	thickness (Å)	ρ (Å^{-2})	σ (Å)	in box	calc.	thickness (Å)	ρ (Å^{-2})	σ (Å)	in box	calc.
PAF 30 mN/m, 20 °C	8.33	0.162	2.6	77	81 (10 C)	12.11	0.406	3.0	281 (incl. ∼6 H_2O)	223
lyso-PAF 30 mN/m, 20 °C	9.79	0.186	3.4	84	81 (10 C)	12.43	0.424	2.5	243 (incl. ∼4 H_2O)	201
lyso-PAF 35 mN/m, 10 °C	12.74	0.197	3.7	89	89 (11 C)	12.35	0.515	2.9	225 (incl. ∼3 H_2O)	193

[a] ρ, electron density; σ, interface roughness.

dx.doi.org/10.1021/jp2121092 | J. Phys. Chem. B 2012, 116, 3155−3163

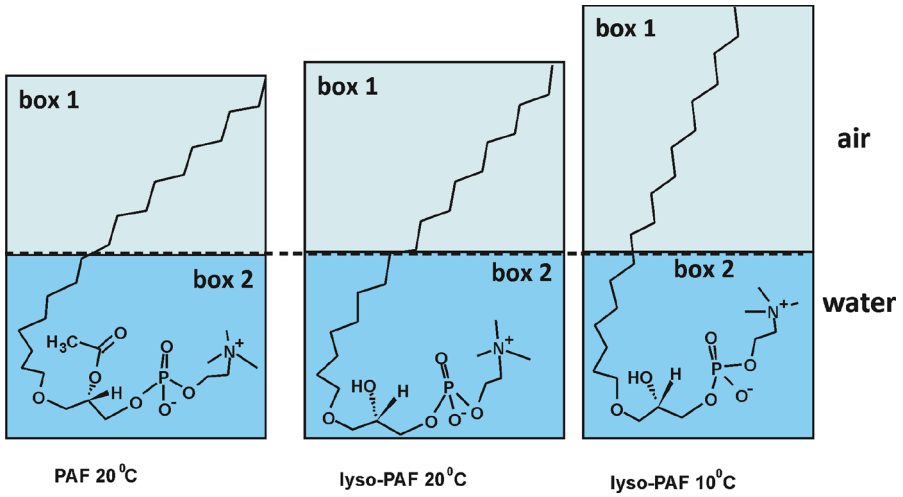

Figure 6. Schematic representation of the orientation of PAF and lyso-PAF molecules at the air/water interface based on parameters obtained from X-ray reflectivity experiments.

~3 water molecules; thus, the degree of hydration practically does not change (Figure 6).

To get a deeper insight into the lateral organization of the investigated single-chained ether lipids molecules in Langmuir monolayers, we decided to apply the grazing incidence X-ray diffraction technique (GIXD). In fact, we were skeptical of this idea, since it is known that monolayers in an expanded state, characterized by low values of compression modulus (<100 mN/m), usually do not provide the 2D diffraction pattern. Indeed, the diffraction signals for monolayers compressed at 20 °C were not acquired. Nevertheless, we decided to repeat the GIXD experiment for the lyso-PAF monolayer compressed to 20 mN/m (below phase transition) and at 35 mN/m (over the phase transition) at 10 °C. Below the phase transition, no diffraction signal was observed, whereas at 35 mN/m it was possible to register a single, weak diffraction signal. The GIXD results are presented in Figure 7.

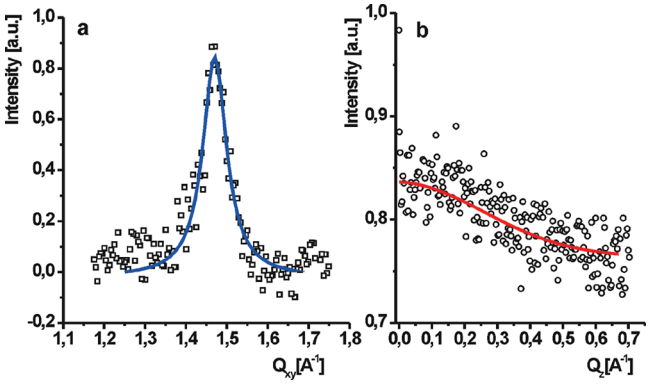

Figure 7. GIXD data registered for the monolayer of lyso-PAF compressed to π = 35 mN/m at 10 °C: (a) diffracted intensity vs in-plane scattering vector Q_{xy} (Bragg peak) and (b) diffracted intensity along the direction perpendicular to the air/water interface (Bragg rod).

For the investigated monolayer, a single broad Bragg peak was acquired with its maximum at Q_{xy} = 1.470 Å^{-1} (Figure 7a). The presence of only one symmetrical Bragg peak visible in the 2D diffractogram indicates that the molecules of lyso-PAF are organized in a hexagonal lattice in the monolayer and are oriented perpendicularly to the air/water interface.[42] The correlation length L_{xy} defined by the Scherrer formula as L_{xy} = 0.9(2π/fwhm) (fwhm is the width of the diffraction peak at half-maximum) is only 80 Å, indicating that the crystalline domains are relatively small. For comparison, L_{xy} calculated for condensed domains in the DPPC monolayer is 209 Å.[53]

It is well-known that the hexagonal lattice is characterized by only one Bragg rod with the maximum localized at $Q_z \sim 0$ Å^{-1} (Figure 7b). The fwhm of the rod is by the Scherrer formula related with the length of the coherently scattering part of the molecule (L_z).[42] For the investigated monolayer, L_z is equal to 10.7 Å. Assuming that this parameter indicates the length of ordered acyl chains, it proves that the film-forming molecules are deeply immersed into the water subphase, as it was previously postulated on the basis of XR experiments.

It can be calculated that in the discussed hexagonal lattice the *d*-spacing is 4.27 Å and therefore the intermolecular distance *a* = 4.93 Å gives the area of the unit cell of 21.08 Å^2. Interestingly, this area differs markedly from the value estimated from the π–*A* isotherm registered for the monolayer of lyso-PAF at this subphase temperature (~34.5 Å^2 per molecule). This discrepancy together with a rather weak intensity of the diffraction peak indicates that only a small fraction of the lyso-PAF molecules is organized in the highly ordered condensed 2D domains, whereas the remaining molecules form the amorphous phase. Although at the considered experimental conditions both phases coexist at the air/water interface, the area calculated from the Bragg peak refers only to the ordered domains.

The situation discussed here is schematically illustrated in Figure 8.

It can be supposed that the crystalline 2D domains float on the sea of the amorphous phase. The phase transition observed in the course of the π–*A* isotherm registered for lyso-PAF monolayers at 10 °C can be correlated with the formation of the crystalline domains. This transition is not reflected in the C_S^{-1}–π dependencies, as only a fraction of the molecules is transformed from the amorphous phase to the crystalline one. Moreover, the crystalline domains do not coalesce to greater 2D crystallites, as no such objects were observed in BAM images which were very similar regardless of the subphase temperature. The propensity of the lyso-PAF molecules to form crystalline domains, and, on the other hand, the lack of such

dx.doi.org/10.1021/jp2121092 | J. Phys. Chem. B 2012, 116, 3155–3163

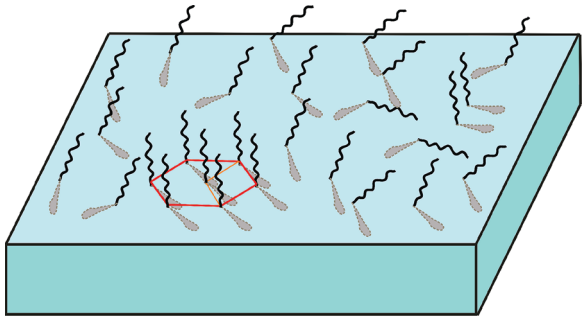

Figure 8. Schematic representation of lyso-PAF molecules in a Langmuir monolayer investigated on a water surface cooled to 10 °C. The red contour indicates a hexagonal arrangement of untilted molecules in highly ordered 2D domains, while the surrounding molecules are involved in the formation of an amorphous phase.

tendency in the PAF monolayers, can be correlated with the presence of the free hydroxyl group in the lyso-PAF molecule. The observed phenomenon is additional evidence of the increased strength of the intermolecular interactions between the lyso-PAF molecules in a model membrane. The involvement of the −OH group in intermolecular hydrogen bonds is highly probable here (but should be corroborated in the future by other independent physicochemical methods). It should be emphasized here that the presence of a free hydroxyl group on the second carbon atom of the headgroup counting from the phosphorus atom makes lyso-PAF similar to the group of sphingolipids. The formation of a hydrogen bond between the headgroup of sphingolipids and other surface active molecules as for example steroids is crucial in the explanation of different phenomena observed for these compounds, e.g., the formation of lipid rafts in cell membranes.[62−64]

CONCLUSIONS

The objective of our studies presented herein was to perform the comparative analysis of two representatives of single-chained ether phospholipids, namely, (C_{18})PAF and its deacetylated precursor (C_{18})lyso-PAF. The motivation of the undertaken experiments comes from the fact that until now relatively little has been known about the properties of the aforementioned lipids at the molecular level. On the other hand, it was well established that both structurally similar phospholipids are substances displaying important, however different in character, physiological activities. Therefore, in our studies, we were looking for the answer concerning the reason for these discrepancies. The results presented in this Article were obtained with the application of the classical Langmuir monolayer technique complemented with the microscopy method (BAM) as well as the synchrotron X-ray reflectivity technique. In preliminary experiments, it was found that both lipids are capable of stable Langmuir monolayer formation. The $\pi-A$ isotherms revealed that the investigated monolayers are of the liquid-expanded (LE) state, whereas the BAM images proved that both surface films are homogeneous upon compression until the values of ESP were reached. First, an important difference in the properties of both lipids was observed in the position of $\pi-A$ isotherms; namely, in the case of lyso-PAF, the curve was significantly shifted toward lower mean molecular areas. Because both lipids have the same hydrophobic fragment, the difference originates from the structure of head-groups. In contrast to PAF, its lyso-analogue possesses a free hydroxyl group localized at the C2 atom of the glycerol backbone, which enables the formation of hydrogen bonds with a neighboring headgroup or with water molecules. This is an important finding, since the possibility of hydrogen bond formation could have important repercussions as far as the behavior of lyso-PAF in biomembranes is concerned. The second discrepancy in characteristics of both lipids is the phase transition in the monolayer of lyso-PAF, which is manifested as a kink visible in the course of the compression isotherm at 20 °C and as a distinct plateau at a lower subphase temperature. The origin of this phenomenon was explained in the GIXD experiment carried out for the lyso-PAF monolayer compressed over the phase transition at 10 °C. Under such conditions, small, highly ordered hexagonal domains are formed, however only from the small fraction of molecules in monolayer. We suggest that the driving force here is the presence of a free −OH group capable of hydrogen bond formation. Our results revealed also that molecules of both PAF and lyso-PAF are strongly immersed into the water subphase, which significantly distinguished them from double-chained phospholipids.[47,61,65]

It can be concluded that our study provides new results regarding the properties of both physiologically active single-chained phospholipids. It is worth mentioning that the experimental parameters investigated herein (temperature, surface pressure) enabled us to highlight important differences in the physicochemical properties of biological potent membrane-active phospholipid: PAF and its structurally similar but less active lyso-derivative. In the near future, we plan also to perform studies regarding the interactions between the above-mentioned single-chained phospholipids and the main lipid components of biological membrane.

AUTHOR INFORMATION

Corresponding Author

*E-mail: flasinsk@chemia.uj.edu.pl.

Notes

The authors declare no competing financial interest.

ACKNOWLEDGMENTS

This project was financed by the National Science Centre (N° DEC-2011/01/B/ST4/00910)

We gratefully acknowledge HASYLAB, DESY (Hamburg) for granting us beamtime at BW1 beamline and would like to express our gratitude to Dr Bernd Struth for his help at BW1.

The research was carried out with the equipment (Ultra-BAM) purchased thanks to the financial support of the European Regional Development Fund in the framework of the Polish Innovation Economy Operational Program (contract no. POIG.02.01.00-12-023/08).

REFERENCES

(1) Farooqui, A. A.; Ong, W.-Y.; Farooqui, T. *Biochim. Biophys. Acta* **2010**, *1801*, 906.

(2) Wang, X.; Devaiah, S. P.; Zhang, W.; Welti, R. *Prog. Lipid Res.* **2006**, *45*, 250.

(3) Magnusson, C. D.; Haraldsson, G. D. *Chem. Phys. Lipids* **2011**, *164*, 315.

(4) McManus, L. M.; Pinckard, R. N. *Crit. Rev. Oral Biol. Med.* **2000**, *11*, 240.

(5) Heymans, F.; Michel, E.; Borrel, M. C.; Wichrowski, B.; Godfroid, J. J.; Convert, O.; Coeffier, E.; Tence, M.; Benveniste, J. *Biochim. Biophys. Acta* **1981**, *666*, 230.

(6) Bussolino, F.; Camussi, G.; Aglietta, M.; Braqeut, P.; Bosia, A; Pescarmona, G.; Sanavio, F.; D'Urso, N.; Marchisio, P. C. *J. Immunol.* **1987**, *139*, 2439.
(7) Ishii, S.; Nagase, T.; Shimizu, T. *Prostaglandins Other Lipid Mediators* **2002**, *68−69*, 599.
(8) Knezevic, I. I.; Predescu, S. A.; Neamu, R. F.; Gorovoy, M. S.; Knezevic, N. M.; Easington, C.; Malik, A. B.; Predescu, D. N. *J. Biol. Chem.* **2009**, *284*, 5381.
(9) Chen, J.; Yang, L.; Foulks, J. M.; Weyrich, A. S.; Marathe, G. K.; McIntyre, T. M. *J. Lipid Res.* **2007**, *48*, 2365.
(10) Esquenazi, S.; Bazan, H. E. P. *Mol. Neurobiol.* **2010**, *42*, 32.
(11) Karabina, S.-A.; Gora, S.; Atout, R.; Ninio, E. *Biochemie* **2010**, 594.
(12) Göggel, R.; Uhlig, S. *Eur. Respir. J.* **2005**, *25*, 849.
(13) Qu, X. W.; Rozenfeld, R. A.; Huang, W.; Crawford, S. E.; Gonzalez, C. F.; Hsueh, W. *J. Physiol.* **1998**, *512*, 227.
(14) Kuebler, W. M.; Yang, Y.; Samapati, R.; Uhlig, S. *Cell. Physiol. Biochem.* **2010**, *26*, 29.
(15) Ferreira, M. A. N. D.; Barcelos, L. S.; Teixeira, M. M.; Bakhle, Y. S.; Andrade, S. P. *Life Sci.* **2007**, *81*, 210.
(16) Denizot, Y.; Gainant, A.; Guglielmi, L.; Bouvier, S.; Cubertafond, P.; Mathonnet, M. *Oncogene* **2003**, *22*, 7222.
(17) Melnikova, V.; Bar-Eli, M. *Cancer Metastasis Rev.* **2007**, *26*, 359.
(18) Braeuer, R. R.; Zigler, M.; Villares, G. J.; Dobroff, A. S.; Bar-Eli, M. *Semin. Cancer Biol.* **2011**, *21*, 83.
(19) Denizot, Y.; Chianea, T.; Labrousse, F.; Truffinet, V.; Delage, M.; Mathonnet, M. *Eur. J. Endocrinol.* **2005**, *153*, 31.
(20) Tsoukatos, D. C.; Brocheriou, I.; Moussis, V.; Panopoulou, C. P.; Christofidou, E. D.; Koussissis, S.; Sismanidis, S.; Ninio, E.; Siminelakis, S. *J. Lipid Res.* **2008**, *49*, 2240.
(21) De Faire, U.; Frostegard, J. *Ann. N. Y. Acad. Sci.* **2009**, *1173*, 292.
(22) Montrucchio, G.; Alloatti, G.; Camussi, G. *Physiol. Rev.* **2000**, *80*, 1669.
(23) Saougos, V. G.; Tambaki, A. P.; Kologirou, M.; Kostapanos, M.; Gazi, I. F.; Wolfert, R. L.; Elisaf, M.; Tselepis, A. D. *Arterioscler., Thromb., Vasc. Biol.* **2007**, *27*, 2236.
(24) Liu, J.; Chen, R.; Marathe, G. K.; Febbraio, M.; Zou, W.; McIntyre, T. M. *Circ. Res.* **2011**, *108*, 469.
(25) Kester, M.; Mene, P.; Dubyak, G. R.; Dunn, M. J. *FASEB J.* **1987**, 215.
(26) Welch, E. J.; Naikawadi, R. P.; Li, Z.; Lin, P.; Ishii, S.; Shimizu, T.; Tirupphathi, C.; Du, X.; Subbaiah, P. V.; Ye, R. D. *Mol. Pharmacol.* **2009**, *75*, 227.
(27) Hąc-Wydro, K.; Dynarowicz-Łątka, P. *J. Phys. Chem. B* **2008**, *112*, 11324.
(28) Wydro, P. *Colloids Surf., B* **2011**, *82*, 594.
(29) McConnell, H, M.; Radhakrishnan, A. *Biochim. Biophys. Acta* **2003**, *1610*, 159.
(30) Dyer, K. D.; Percopo, C. M.; Xie, Z.; Yang, Z.; Kim, J. D.; Davoine, F.; Lacy, P.; Druey, K. M.; Moqbel, R.; Rosenberg, H. F. *J. Immunol.* **2010**, *184*, 6327.
(31) Isomaa, B.; Hagerstrand, H.; Paatero, G. *Biochim. Biophys. Acta* **1987**, *899*, 930.
(32) Hagerstrand, H.; Isomaa, B. *Chem.-Biol. Interact.* **1991**, *79*, 335.
(33) McIntyre, T. M.; Prescott, S. M.; Stafforini, D. M. *J. Lipid Res.* **2009**, *50*, S255.
(34) Föller, M.; Huber, S. M.; Lang, F. *IUBMB Life* **2008**, *60*, 661.
(35) Mrówczyńska, L.; Hägerstrand, H. *J. Biochem. Mol. Toxicol.* **2009**, *23*, 345.
(36) Gajate, C.; Mollinedo, F. *Curr. Drug Metab.* **2002**, *3*, 491.
(37) Wieder, T.; Reutter, W.; Orfanos, C. E.; Geilen, C. C. *Prog. Lipid Res.* **1999**, *38*, 249.
(38) Gajate, C.; del Canto-Jañez, E.; Ulises Acuña, A.; Amat-Guerri, F.; Geijo, E.; Santos-Beneit, A. M.; Veldman, R. J.; Mollinedo, F. *J. Exp. Med.* **2004**, *200*, 353.
(39) Kjaer, K. *Physica B* **1994**, *198*, 100.
(40) Als − Nielsen, J.; Jacquemain, D.; Kjaer, K.; Leveiller, F.; Lahav, M.; Leiserovitz, L. *Phys. Rep.* **1994**, *246*, 251.
(41) *Modern characterization methods of surfactant systems*; Binks, B. P., Ed.; Marcel Dekker, Inc.: 1999.
(42) *Novel method to study interfacial layers*; Möbius, D., Miller, R., Eds.; Elsevier: 2001.
(43) Lee, K. Y. C.; Majewski, J.; Kuhl, T. L.; Howes, P. B.; Kjaer, K.; Lipp, M. M.; Waring, A. J.; Zasadzinski, J. A.; Smith, G. S. *Biophys. J.* **2001**, *81*, 572.
(44) Parratt, L. G. *Phys. Rev.* **1954**, *93*, 359.
(45) Flasiński, M.; Broniatowski, M.; Majewski, J.; Dynarowicz-Łątka, P. *J. Colloid Interface Sci.* **2010**, *348*, 511.
(46) Broniatowski, M.; Flasiński, M.; Dynarowicz-Łątka, P.; Majewski, J. *J. Phys. Chem. B* **2010**, *114*, 12549.
(47) Broniatowski, M.; Flasiński, M.; Dynarowicz-Łątka, P.; Majewski, J. *J. Phys. Chem. B* **2010**, *114*, 9474.
(48) Hąc-Wydro, K.; Flasiński, M.; Broniatowski, M.; Dynarowicz-Łątka, P.; Majewski, J. *J. Phys. Chem. B* **2010**, *114*, 6866.
(49) Majewski, J.; Stec, B. *Eur. Biophys. J.* **2010**, *39*, 1155.
(50) Davies, J. T.; Rideal, E. K. *Interfacial Phenomena*: Academic Press: New York and London, 1963.
(51) Gambinossi, F.; Puggelli, M.; Gabrielli, G. *Colloids Surf., B* **2002**, *23*, 273.
(52) Rodriguez Niño, M. R.; Lucero Caro, A.; Rodriguez Patino, J. M. *Colloids Surf., B* **2009**, *69*, 15.
(53) Gonçalves da Silva, A.; Romão, R. S.; Lucero Caro, A.; Rodriguez Patino, J. M. *J. Colloid Interface Sci.* **2004**, *270*, 417.
(54) Broniatowski, M.; Vila-Romeu, N.; Nieto-Suarez, M.; Dynarowicz-Łątka, P. *J. Phys. Chem. B* **2007**, *111*, 12787.
(55) Osak, A.; Dynarowicz-Łątka, P.; Conde, O.; Minones, J. Jr.; Pais, S. *Colloids Surf., A* **2008**, *319*, 71.
(56) Carrera Sanchez, C.; Rodriguez Niño, M. R.; Rodriguez Patino, J. M. *Colloids Surf., B* **1999**, *12*, 175.
(57) Miller, C. E.; Busath, D. D.; Strongin, B.; Majewski, J. *Biophys. J.* **2008**, *95*, 3278.
(58) Schalke, M.; Krüger, P.; Weygand, M.; Lösche, M. *Biochim. Biophys. Acta* **2000**, *1464*, 113.
(59) Stengert, P. C.; Wu, G.; Miller, C. E.; Chi, E. Y.; Frey, S. L.; Lee, K. Y. C.; Majewski, J.; Kjaer, K.; Zasadzinski, J. A. *Biophys. J.* **2009**, *97*, 777.
(60) Tanford, C. *The Hydrophobic Effect*; Wiley: New York, 1973.
(61) Naumann, C.; Brumm, T.; Rennie, A. R.; Penfold, J.; Bayerl, T. M. *Langmuir* **1995**, *11*, 3948.
(62) Simons, K.; Ikonen, E. *Nature* **1997**, *387*, 569.
(63) Radhakrishnan, A.; McConnell, H. M. *Biophys. J.* **1999**, *77*, 1507.
(64) Jablin, M. S.; Flasiński, M.; Dubey, M.; Ratnaweera, D. R.; Broniatowski, M.; Dynarowicz-Łątka, P.; Majewski, J. *Biophys. J.* **2010**, *99*, 1475.
(65) Helm, C. A.; Tippmann-Krayer, P.; Möhwald, H.; Als-Nielsen, J.; Kjaer, K. *Biophys. J.* **1991**, *60*, 1457.